Characterization of Peptide Adsorption on InAs Using X-ray Photoelectron Spectroscopy

ARTICLE *in* LANGMUIR · MARCH 2011

Impact Factor: 4.46 · DOI: 10.1021/la104963v · Source: PubMed

3 AUTHORS, INCLUDING:

Dmitry Zemlyanov
Purdue University
132 PUBLICATIONS **1,802** CITATIONS
SEE PROFILE

Albena Ivanisevic
North Carolina State University
112 PUBLICATIONS **1,204** CITATIONS
SEE PROFILE

Langmuir

ARTICLE

pubs.acs.org/Langmuir

Characterization of Peptide Adsorption on InAs Using X-ray Photoelectron Spectroscopy

Scott Jewett,[†] Dmitry Zemlyanov,[‡,§] and Albena Ivanisevic[†,∥,*]

[†]Weldon School of Biomedical Engineering, [‡]Birck Nanotechnology Center, [§]Department of Chemical Engineering, and [∥]Department of Chemistry, Purdue University, West Lafayette, Indiana 47907, United States

Supporting Information

ABSTRACT: The well-defined structure and high stability of peptides make them attractive biotemplates for low-temperature synthesis of semiconductor nanocrystals. Adsorbed peptide monolayers could also potentially passivate semiconductors by preventing regrowth of the oxide layer. In this work, the adsorption and passivation capabilities of different collagen-binding peptides on InAs surfaces were analyzed by X-ray photoelectron spectroscopy (XPS). Before peptide functionalization, Br_2- and HCl-based etches were used to remove the native oxide layer on the InAs surfaces. The presence of the N 1s peak for peptide-functionalized samples confirms the adsorption of peptides onto the etched InAs surfaces. Calculated coverages were similar for all peptide sequences and ranged from ~20 to 40% of a monolayer using the deconvoluted C 1s spectra and from ~2 to 5% for the N 1s spectra. The passivation ability of the peptides was analyzed by comparing the ratios of the oxide components to the nonoxide components in the XPS spectra. The thickness of the oxide layer was also approximated by accounting for the attenuation of the substrate photoelectrons through the oxide layer. We find that the oxide layer regrowth still occurs after peptide functionalization. However, the oxide layer thicknesses for peptide-functionalized samples do not reach as received levels, indicating that the peptides do have some passivation ability on InAs.

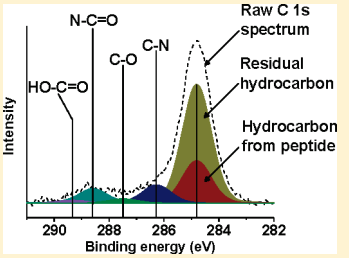

INTRODUCTION

Group III−V semiconductors have received considerable attention for use in applications such as nanosized electronic devices, biochemical and chemical sensors, and high-speed field effect transistors (FETs). Indium arsenide (InAs) is a III−V semiconductor that is particularly attractive in high-speed electronics[1,2] and chemical sensing[3] because of its unique electronic properties. Due to its small bandgap, surface states can have a dramatic effect on the electronic properties of InAs. As such, surface adsorbates that alter the charge character of surface states in turn lead to high sensitivity of InAs to biological or chemical species. Device effectiveness, therefore, is highly dependent on the purity and stability of the semiconductor surface. Thus, minimization of outside contaminants is a key factor in the design of all InAs-based devices. This poses a problem, because in ambient or aqueous conditions, oxide growth and unwanted molecular contamination can cause instability and wreak havoc on overall device function. One common way of stabilizing semiconductor surfaces is by surface passivation through the adsorption of self-assembled monolayers (SAMs), which act as a protective barrier against contaminants and oxide growth, while still allowing for device function. Simple alkanethiols have emerged as particularly attractive to passivate InAs surfaces and have received the bulk of attention in the literature.[3−6] Alkanethiols have a relatively high affinity for InAs, and they have been shown to preserve or even improve the electronic properties of InAs.[7,8]

However, several applications of III−V semiconductors require modification with more complex biomolecules. There have been several reports of using DNA in conjunction with III−V semiconductors for sensing applications,[9−11] but there is also much interest in using biomolecules as templates to assemble or grow nanostructures. Viruses,[12−14] DNA,[15−17] and peptides[18−24] offer consistent, well-defined structures that allow for the assembly of nanostructures in relatively mild conditions. Most applications use self-assembly to form hierarchal nanostructures, but with the advent of low-temperature nanocrystal growth techniques, such as the solution−liquid−solid[25,26] (SLS) method, it is also possible to use biomolecules as templates for the growth of *single nanocrystal* structures. Peptides are particularly promising biotemplates for nanocrystal growth. For example, one group demonstrated the growth of ZnO nanocrystals catalyzed by a collagen-mimetic peptide, which was engineered to withstand high pH levels.[18] Despite the wealth of applications, the exact mechanism of peptide/III−V semiconductor binding remains unknown.

The binding of peptides to III−V semiconductors has been of particular interest for the past decade and began with using phage libraries to select peptides with high affinities for GaAs.[24] Atomic force microscopy (AFM) and X-ray photoelectron spectroscopy (XPS) studies indicate that peptide binding to semiconductors is most likely mediated by both the charge[24] and order[27,28] of the peptide amino acid structure. Additionally, AFM studies show

Received: December 14, 2010
Revised: February 25, 2011
Published: March 14, 2011

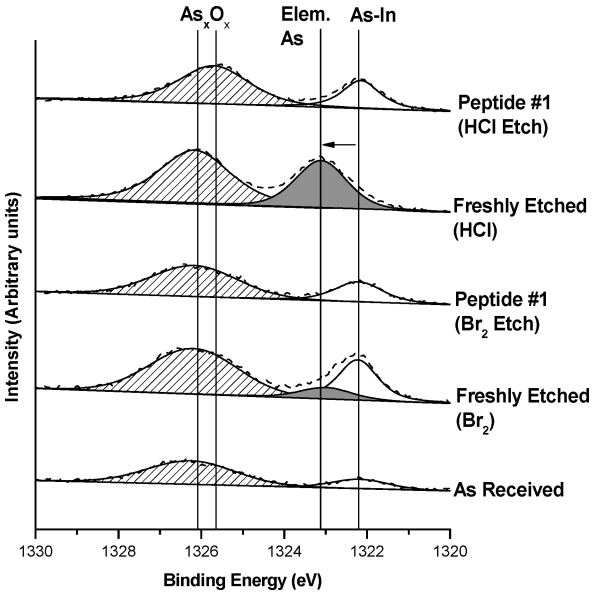

Figure 1. As $2p_{3/2}$ spectra of InAs samples. The As−In component is located at ∼1322.2 eV. The freshly HCl etched surface displays significant elemental arsenic contamination at 1323.1 eV. The freshly Br_2-etched sample displays a minimal elemental arsenic contamination. The As_xO_x components are present at 1326.2 and 1325.7 eV.

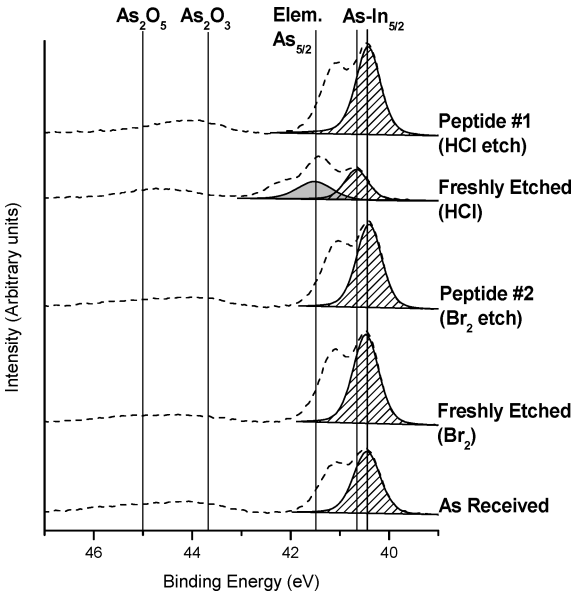

Figure 2. As 3d spectra of InAs samples. Both elemental arsenic (41.5 eV) and As−In (∼40.5 eV) are present in the freshly HCl-etched surface. The two arsenic oxide components, As_2O_3 and As_2O_5, are present at ∼43.7 and ∼45 eV. A doublet separation of 0.68 eV was used to separate the As $3d_{5/2}$ and As $3d_{3/2}$ components.

that peptides do not form well-defined monolayers on semiconductors but agglomerate to form clusters, with larger and higher clusters indicative of decreased affinity to the semiconductor.[27,28] Many of the reports involving nonthiolated peptide/semiconductor interactions are more qualitative, and the exact nature of the peptide/semiconductor binding has not been thoroughly investigated by XPS. Because of the wealth of applications, from passivation to biotemplates for nanocrystal growth, it is important to perform a detailed assessment of the binding of peptides to semiconductors. In this report, we use XPS to assess the adsorption of different collagen-binding peptides on InAs surfaces. We have two main goals in this study: to determine the success of the peptide adsorption on InAs in terms of peptide monolayer coverage and to analyze the passivation ability of the peptides through approximating the regrowth of the oxide layer.

EXPERIMENTAL DETAILS

Sample Preparation. Undoped InAs(100) samples (∼0.5 cm^2) were first cleaned by sonicating for 15 min in Milli-Q water, methanol, and ethanol and then dried with N_2. Cleaned samples were then etched to remove the native oxide layer using either a Br_2- or HCl-based etch. The Br_2 etch solution consisted of as received Br_2 (99%, Sigma) diluted in methanol to 0.1% volume concentration. Samples were incubated in the Br_2 solution for 3 min; sonicated for 5 min in Milli-Q water, methanol, and ethanol; and then dried with N_2. The HCl etch was performed by diluting the as received HCl (11.65 M, Sigma) in 2-propanol to a 3 M concentration. Samples were incubated for 1 min, rinsed twice with 2-propanol, and then dried with N_2. Samples were then annealed in an oven for 10 min at 250 °C.

After etching, samples were immediately transferred to 10 μg/mL peptide solutions diluted in PBS and incubated at room temperature for 2 h. Samples were then rinsed with Milli-Q water and incubated in a Milli-Q water bath for 20 min, to remove all unbound or loosely bound peptide, and then dried with N_2. The peptide sequences included a collagen-binding peptide, GCGGELYKSILY (P1), along with three variants of this peptide, GCGGELYASILY (P2), GCGGELAKSILY (P3), and GCGGELYKSILA (P4), which contain single point alanine substitutions. The final peptide had the sequence INPISGQGC (P5). Peptides P1 and P5 were synthesized using solid-phase synthesis, as described previously,[29] while peptides P2−P4 were purchased from GenScript.

To minimize reoxidation, freshly etched samples were immediately transported to the XPS analyzer after etching. However, there was contact with ambient air during transport, so some reoxidation of the freshly etched samples was expected. As received samples were cleaned by sonicating for 15 min in Milli-Q water, methanol, and ethanol before XPS analysis. Peptide functionalized samples were stored at room temperature for several weeks until XPS analysis.

X-ray Photoelectron Spectroscopy. X-ray photoelectron spectroscopy data was obtained with a Kratos Ultra Axis DLD spectrometer using an Al Kα monochromatic X-ray radiation (1486.6 eV). Both survey and high resolution spectra were collected at 0° with respect to the surface normal at pass energies of 20 and 160 eV, respectively. The high-resolution spectra included As 2p, O 1s, In 3d, N 1s, C 1s, S 2p, As 3d, and In 4d core levels. Charge correction was performed using the C 1s peak at 284.80 eV. Data analysis was performed using the CasaXPS software, version 2.3.12. Gaussian−Lorentzian line shapes were used to fit the data, and the background was modeled using either Shirley or Linear functions.

Atomic Force Microscopy. Samples were imaged in tapping mode using a Digital Instruments Multi-Mode Nanoscope IIIa atomic force microscope. Scan sizes ranged from 2 to 4 μm, with imaging speeds of 2−3 Hz. Images were analyzed with the Nanoscope III 5.12r5 software and processed using a zero- or first-order flattening.

RESULTS AND DISCUSSION

Analysis of Freshly Etched Surfaces. In ambient conditions, untreated semiconductor surfaces form oxide components that can be removed through surface etching. In this study, both Br_2- and HCl-based etches were used to remove the outer oxide layer

dx.doi.org/10.1021/la104963v |*Langmuir* 2011, 27, 3774–3782

Table 1. Ratios of Oxide to Non-Oxide Components for Each Sample

sample[a]	As $2p_{3/2}$	As 3d	In 3d	In 4d
as received	4.0	0.32	1.0	0.82
freshly HCl etched[b]	–	–	–	–
P1 (HCl etch)	2.6	0.28	0.83	0.69
P2 (HCl etch)	2.8	0.26	0.85	0.73
P3 (HCl etch)	2.7	0.24	0.89	0.71
P4 (HCl etch)	1.8	0.21	0.76	0.68
P5 (HCl etch)	3.0	0.24	0.86	0.67
freshly Br_2 etched	1.6	0.17	0.54	0.47
P1 (Br_2 etch)	3.7	0.24	0.87	0.63
P2 (Br_2 etch)	2.5	0.22	0.84	0.68
P3 (Br_2 etch)	3.2	0.26	0.91	0.72
P4 (Br_2 etch)	2.5	0.20	0.78	0.61
P5 (Br_2 etch)	3.2	0.26	0.95	0.77

[a] P1–P5 correspond to samples functionalized with peptides P1 through P5. [b] Not shown because of difficulty in deconvoluting the spectra.

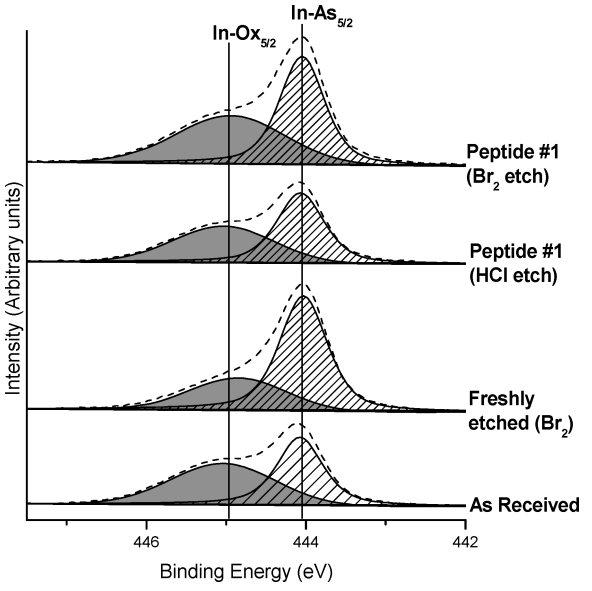

Figure 3. In $3d_{5/2}$ spectra of InAs samples. The In–As peak is located at ~444.1 eV and the In_2O_3 peak is located at ~444.9 eV. Note that the freshly HCl-etched surface is not shown because of the difficulty in deconvoluting the spectrum due to contamination.

and expose the InAs surface. To determine the success of the oxide removal, the presence of the oxide components was analyzed in the As $2p_{3/2}$, As 3d, In 3d, and In 4d spectra (Figures 1–4). We have acquired the As $2p_{3/2}$ and As 3d regions for arsenic characterization and the In 3d and In 4d spectra for indium. The As $2p_{3/2}$ peak has a binding energy (BE) of ~1325 eV, which corresponds to a photoelectron kinetic energy (KE) of ~160 eV. For the As 3d peak, the BE and KE are ~41 and 1445 eV, respectively. The difference in the KE of the As $2p_{3/2}$ and As 3d photoelectrons results in a different electron attenuation length (EAL), and therefore, the As $2p_{3/2}$ and As 3d spectra have different surface sensitivities. The same consideration is applied for the In 3d and In 4d spectra. It is important to note that

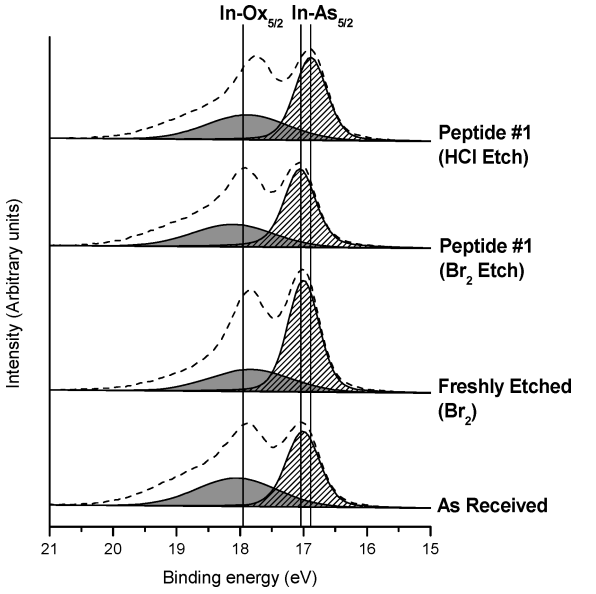

Figure 4. In $4d_{5/2}$ spectra of InAs samples. The In–As peak is located at ~17 eV and the In_2O_3 peak is located at ~18 eV. Note that the freshly HCl-etched surface is not shown because of the difficulty in deconvoluting the spectrum due to contamination.

in Figure 2 only the As $3d_{5/2}$ components are labeled. Since a doublet separation of 0.68 eV was used, the As $3d_{3/2}$ components are located +0.68 eV from their respective As $3d_{5/2}$ components. For example, the peak at ~41.2 eV in Figure 2 represents the As–$In_{3/2}$ component.

The oxide components present in the samples included In_2O_3, As_2O_3, and As_2O_5, while the nonoxide components included In–As or As–In. Ideally, the freshly Br_2-etched sample would have no oxide components; however, despite the etching, the freshly Br_2 etched sample showed the presence of oxide components in the As $2p_{3/2}$, As 3d, In 3d, and In 4d spectra (Figures 1–4). Since there was contact with ambient air between etching and XPS analysis, some reoxidation of the sample is expected. The relative oxidation of the samples was determined by analyzing intensity ratios between the oxide and nonoxide components in the As $2p_{3/2}$, As 3d, In 3d, and In 4d XPS spectra, which are summarized in Table 1. The ratios are different for components in the As $2p_{3/2}$, As 3d, In 3d, and In 4d core levels, because the different surface sensitivity of the core levels. The ratio of the oxide components to the nonoxide components was significantly lower for the Br_2-etched sample than the as received sample, indicating that there was removal of the outer oxide layer and a greater exposure of the InAs after etching. Importantly, during peptide adsorption, there was no lag time between etching and peptide functionalization, so it is reasonable to conclude that there were minimal oxide components on the InAs surface during the peptide functionalization step. Minimal contamination in the form of elemental arsenic was present on the Br_2-etched surface, based on the presence of a small peak at ~1323 eV in the As $2p_{3/2}$ spectrum (Figure 1).

Halogens are notoriously toxic and can be difficult to work with as pure substances. Furthermore, pure halogen-based etches can be physically destructive to the semiconductor surface, causing the formation of large pits during the etching process.[30] Acid-based etches can provide a somewhat gentler alternative to pure halogen-based etches. In this study, we also used an HCl/2-propanol

dx.doi.org/10.1021/la104963v |*Langmuir* 2011, 27, 3774–3782

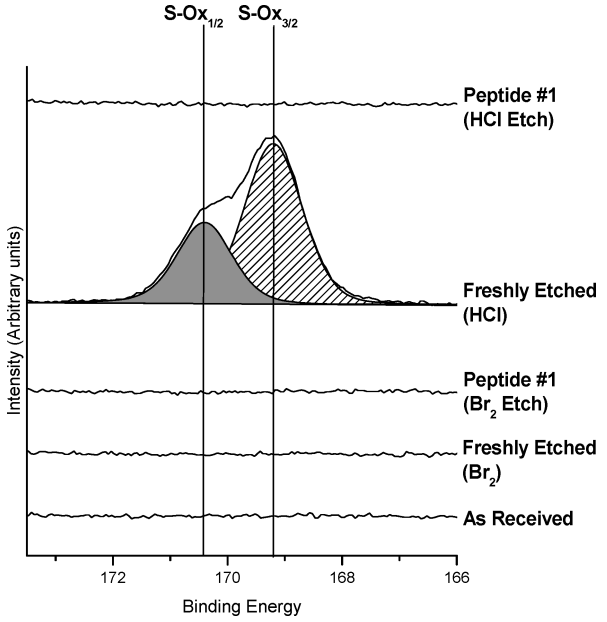

Figure 5. S 2p spectra of InAs samples. The freshly HCl-etched sample displays significant sulfur oxide contaminants at 169.2 and 170.4 eV. The remainder of the samples showed no visible components in the S 2p spectra.

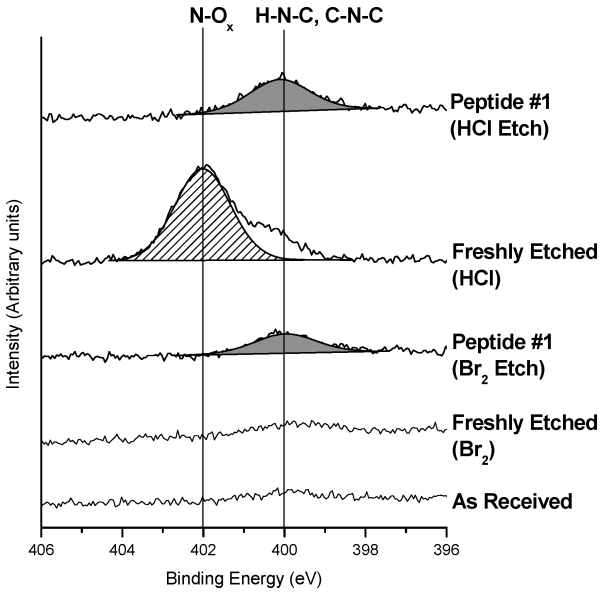

Figure 6. N 1s spectra of InAs samples. The freshly HCl-etched sample displays significant nitrogen oxide contamination at 402 eV. The amine peaks at ~400 eV indicates adsorption of peptide onto the InAs surfaces.

solution as an acidic etch to remove the outer oxide layer, followed by a short annealing step to remove any adsorbed contaminants. As seen by Figures 5 and 6, the freshly HCl etched sample displayed significant contamination in the form of nitrogen and sulfur oxides at ~402 and 170.4 eV, respectively. The presence of these oxides is confirmed by a nearly 3-fold increase in area in the O 1s intensity as compared with other samples (data not shown). A significant amount of elemental arsenic was also found in the freshly HCl-etched surface, as indicated by the shift of the peak in the As $2p_{3/2}$ spectra from 1322.2 eV (As−In) to 1323.1 eV (elemental arsenic) (Figure 1), along with an elemental arsenic component in the As 3d spectra at 41.5 eV (Figure 2). The kinetic energy of the As $2p_{3/2}$ spectrum is relatively low (158−166 eV), so the As $2p_{3/2}$ spectrum is representative of the elements on the outermost surface layer of the sample. Since the As $2p_{3/2}$ spectrum indicates minimal As−In binding at 1322.2 eV, elemental arsenic most likely formed a thin layer on the top of the InAs surface, along with nitrogen oxide and sulfur oxide contaminants. This is confirmed by the presence of both As−In and elemental arsenic components in the As 3d spectra (40.5 and 41.5 eV, respectively), which at a high KE (~1446 eV) penetrates deeper into the InAs surface. Previous reports suggest that acidic etches cause elemental arsenic and oxide contamination;[4,31,32] however, the contaminants are usually removed through annealing. In terms of oxide removal ratios (Table 1), it is difficult to resolve the oxide components in the As 3d, In 3d, and In 4d spectra because of contamination; therefore, it is difficult to accurately determine the oxide ratios for the freshly HCl-etched surface.

The goal of this study is not necessarily to analyze the effect of different etches on InAs, but there are several conclusions that can be made on the basis of the data. First, in terms of the HCl etch, the temperature of our annealing step was lower than other anneal temperatures involving InAs, suggesting that the anneal temperature plays a critical role in removal of the surface contaminants. Detailed analyses of the anneal temperature suggest that a temperature of over 400 °C is necessary to completely remove physioadsorbed contaminants and create a bare, indium-rich InAs surface. However, these reports suggest that regardless of the anneal temperature, HCl etches do completely remove the indium and arsenic oxide layers, despite the presence of adsorbed contaminants.[4,31,32] On the basis of our data, the Br_2 etch produces more consistent etching results both in terms of oxide removal and reduction of contamination. Additionally, despite being a more difficult substance to work with, the Br_2 etch does not require an additional high-temperature annealing step. We also did not see any visible evidence of pit formation on the InAs surface, which could be attributed to the low (0.1%) concentration of Br_2 and the short exposure time (3 min) used in our experiments.

Notes on Peptide Binding. To determine the presence of the peptide on the InAs surface, we compared the intensities of the N 1s spectra of as received and etched surfaces to the peptide-functionalized surfaces. For all peptide-functionalized samples, the intensities of the N 1s spectra increased compared to the as received and freshly Br_2-etched surfaces. Additionally, the increase occurred at ~400 eV in the N 1s spectra, which is indicative of the amide and amine compounds (Figure 6). While there was an increase in N 1s intensity, this increase was relatively small, indicating that only a small amount of peptide actually adsorbed on the surface. There is also some concern that, on the basis of the S 2p peak, there is no sulfur found on the peptide-functionalized samples, despite the presence of cysteine in the peptide sequences. In the peptide structures, there was more than a 10:1 ratio of nitrogen to sulfur atoms; therefore, because of the small increase in N 1s intensity, it is likely that sulfur content is below the XPS detection limit.

Since all samples were subjected to rigorous postfunctionalization washing, the peptide must be tightly bound to the surface. We therefore also investigated the nature of binding of the peptide to the InAs surface. Previous reports have been inconclusive on the nature of binding of peptides to semiconductors,

Table 2. Number, Type, and Binding Energies of Carbon Atoms Present in Each Peptide Structure

	C−C, C−H, or C−S type 1	C−N type 2	C−O type 3	O═C−N type 4	O═C−OH type 5
P1	29	13	3	11	2
P2	28	12	3	11	2
P3	25	13	2	11	2
P4	25	13	2	11	2
P5	14	10	1	10	1
BE (eV)	284.8	285.5−286.5	286.4−287.4	287.4−288.6	288.5−289.6

but it is believed that charged or polar amino acids play some role in peptide/semiconductor binding. Thiol-based SAMs have been shown to bind to InAs primarily through In−S binding;[4,6,7] so because of the presence of a cysteine in the peptides, we first searched for In−S or As−S binding components. In the In 3d spectrum, the In−S binding component is normally found at ∼445 eV. However, the In_2O_3 component binding energy differs from the In−S by only ∼0.2 eV, making it difficult to accurately distinguish between the two components. Since there is a component peak present at ∼445 eV for the freshly Br_2 etched sample (Figure 3), it is most likely that the 445 eV peak found in the peptide-functionalized sample is indicative only of In_2O_3 and not In−S. Therefore, for both the HCl- and Br_2-etched peptide-functionalized samples, we detected no In−S binding in the In 3d spectra. In the As 2p spectra, there was a consistent component at 1325.9 eV for all HCl-etched surfaces, which could be indicative of As−S binding (Figure 1). This peak shift is not present in the Br_2-etched samples or in the as received sample. However, it is also possible that this peak is due to residual sulfur oxides bound to the elemental arsenic, or because of the close proximity to the As_2O_3 component, the shift could represent some form of arsenic oxide. The consistency of the peak at 1325.9 eV throughout the HCl-etched peptide-functionalized samples most likely indicates that the oxide layer is different in composition than the Br_2-etched peptide-functionalized samples, but it is difficult to make a definitive conclusion based on the current information.

Aside from the cysteine, other potential sites include the charged and polar amino acids present in the peptides, including lysine, tyrosine, asparagine, and glutamine. There are also previous reports of amine groups binding with arsenic atoms in GaAs.[10,11] This was tested by substituting an uncharged alanine amino acid for lysine in P2 and tyrosine in P3 and P4. Overall, there were no consistent differences in N 1s intensity and peptide coverage between any of the peptides, suggesting that neither the lysine nor tyrosines played a significant role in binding. Furthermore, since there is only a single lysine in peptides P1, P3, and P4, it is unlikely that the binding through the amine occurred. Finally, P5 contained a glutamine and asparagine and displayed no change in binding or coverage when compared with P1−P4, suggesting that neither glutamine nor asparagine played a role in peptide binding. Overall, the lack of binding evidence combined with the overall lack of free amines and thiols in the peptides make it unlikely that either were the primary means of binding the peptides to the InAs surface.

With the data from this study, it remains difficult to make definitive conclusions on peptide/semiconductor binding. It is unlikely that the peptides formed nitrogen or sulfur covalent bonds to the InAs surface, based on the lack of In−S components and the similarities in adsorption between P1 and the lysine-free P2. The relatively long length of the peptides (9−12 amino acids) most likely causes the peptides to be conformed in a manner that prevents the thiol or amine groups on the peptide from being exposed enough to bind to the InAs. Although there was no evidence of sulfur or nitrogen covalent bonding, the peptides remained on the surface even after rigorous washing, indicating that the peptides were tightly bound to the InAs. Aside from nitrogen or sulfur, another possible mode of binding would be through oxygen or carbon molecules, both of which are abundant in peptides. Both oxygen and carbon have higher electronegativities than indium and arsenic, raising the possibility of the formation of an electrostatic bond with the exposed indium or arsenic. Unfortunately, with the current information, it is difficult to determine the exact mode of peptide/semiconductor binding.

Peptide Curve Fitting. The C 1s high-resolution spectrum has been shown to give an accurate fingerprint of peptide adsorption.[33] The central idea behind the C 1s deconvolution is to correlate the chemical state of the carbon atoms in the peptide structure to components observed in the C 1s spectra. The peak intensity of carbon atoms in the different chemical states is linearly proportional to the number of the atoms in the given chemical state. This fact can be used for a curve-fitting. There are five distinct chemical states of carbon present in the peptide structure, which correspond to distinct chemical shifts in the C 1s peak. Type 1 includes carbon bonded only to carbon or hydrogen molecules. Type 2 represents carbon bonded to a single nitrogen atom along with a carbon or hydrogen, as in lysine. Type 3 carbons are single bonded to a single oxygen atom, as in tyrosine or serine. Type 4 carbons are from amide groups in each peptide bond. Type 5 represents the carbon present in a carboxylic acid group. Due to the cysteine amino acid, there is also carbon bound to sulfur present in the peptides, but because of the proximity of the binding energies, we combined carbon−sulfur with type 1 carbons. The number and type of carbon molecules, along with their corresponding binding energies, are summarized in Table 2. The ratios between type 1 carbons and types 2−5 were then determined, and these ratios were set as constants in the Casa XPS software. Another peak was then added at 284.8 eV to account for residual hydrocarbons. During the subsequent calculations for peptide coverage, the area of the residual hydrocarbons was subtracted. Throughout C 1s curve fitting, all peak widths were kept identical. The peak locations were restricted by the binding energy values given in Table 2. The structure and carbon labeling of P1, along with the exact area ratios used, are shown in the Supporting Information. Figure 7 shows a fully deconvoluted C 1s spectrum for the P1 HCl etched sample.

Peptide Coverage. After using the N 1s spectra to confirm that the peptide is adsorbed on the InAs surface, the C 1s and N 1s spectra can be used to calculate peptide coverage for each sample. The peptide adlayer is assumed to be a nonattenuating overlayer as outlined by Fadley,[34] and the coverage can be calculated using the following equation (for complete derivation, see the Supporting Information):

$$\Theta = \frac{\frac{d\sigma_s}{d\Omega}\Lambda_e^{subst}(E_s)\,N_l(\theta)}{\frac{d\sigma_l}{d\Omega}\,dN_s(\theta)} \quad (1)$$

dx.doi.org/10.1021/la104963v |*Langmuir* 2011, 27, 3774–3782

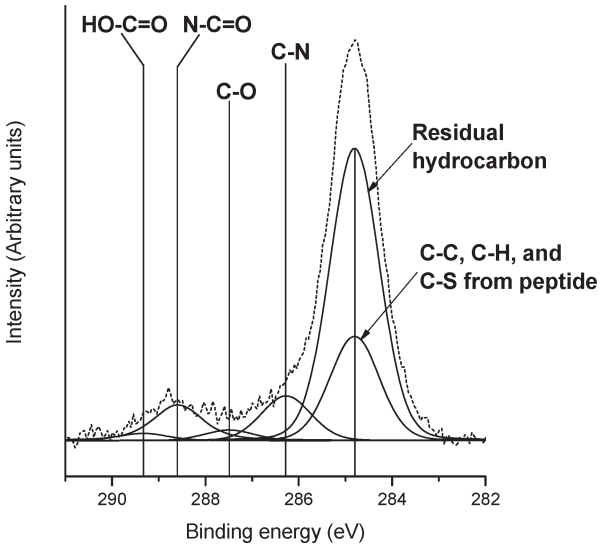

Figure 7. Deconvolution of the C 1s spectrum for P1, HCl-etched sample. The ratios for the areas of each component were adjusted on the basis of peptide atomic structure.

In the calculations, the coverage, Θ, is defined as the number of peptide molecules per either indium or arsenic atoms on the surface; $d\sigma_s/d\Omega$ is a differential cross-section for In 3d or As 3d photoemission lines depending on the tabulated Scofield relative sensitivity factor corrected for the Reilman asymmetric parameter; $d\sigma_l/d\Omega$ is a differential cross-section of the C 1s or N 1s photoemission lines; Λ_e^{subst} is the inelastic mean free pass (IMFP) of the In 3d or As 3d photoelectrons through InAs; $N_l(\theta)$ is the intensity of the peptide component of the C 1s or N 1s spectrum; $N_s(\theta)$ is the intensity of the In−As component in the In 3d peak or the As−In component in the As 3d spectra; and d is the distance between the closest plane of In/As(100), which is half of the lattice constant of InAs, 3.03 Å. As discussed by Jablonski and Powell,[35] the IMFP can be replaced with electron attenuation lengths for quantitative analysis (QEAL) as calculated by the NIST SRD 82 software.[36]

As seen in Table 3, the peptide coverages range from ∼20 to 0% of a monolayer for the C 1s spectra and from ∼2 to 5% of a monolayer for the N 1s spectra. Such a stark difference between the two spectra is most likely caused by the presence of carbon oxide contamination on the InAs substrates, which were present even on the as received and freshly Br_2 etched samples (data not shown). For the peptide curve fitting, there was no way to ensure that the carbon oxides were only indicative of peptide and not carbon oxide contamination. This contamination likely inflated the peptide coverage as calculated by the C 1s spectra. The peptide coverages for the In 3d and As 3d photoemission lines were very similar, with the As 3d slightly higher than the In 3d for both C 1s and N 1s. In our experiments, we saw consistent arsenic depletion on the surface of the substrate based on indium and arsenic atomic percentages. Therefore, the consistently higher peptide coverages for As 3d peak are most likely due to a depletion of arsenic on the InAs near-surface region that can occur after exposure to etching or passivation solutions, as described previously.[37] When comparing the peptide coverages, there are no consistent differences between surface coverage using either the C 1s or N 1s spectra. Therefore, based on these calculations, there is no evidence to suggest that there is any difference in coverage based on peptide sequence.

Table 3. Estimated Peptide Coverage Using the In 3d and As 3d Peaks

	calculated using C 1s spectra		calculated using N 1s spectra	
	molecules per In atom (In 3d)	molecules per As atom (As 3d)	molecules per In atom (In 3d)	molecules per As atom (As 3d)
P1 (HCl etch)	0.29	0.34	0.02	0.02
P2 (HCl etch)	0.26	0.27	0.03	0.03
P3 (HCl etch)	0.22	0.23	0.03	0.03
P4 (HCl etch)	0.22	0.25	0.02	0.02
P5 (HCl etch)	0.30	0.33	0.04	0.05
P1 (Br_2 etch)	0.28	0.29	0.03	0.04
P2 (Br_2 etch)	0.32	0.36	0.04	0.05
P3 (Br_2 etch)	0.37	0.37	0.04	0.05
P4 (Br_2 etch)	0.27	0.32	0.03	0.04
P5 (Br_2 etch)	0.18	0.20	0.04	0.05

Table 4. Estimated Thicknesses of the Oxide Layers Calculated Using the In_2O_3, As_2O_3, or As_2O_5 Component Intensities

	In_2O_3 (Å)	As_2O_3 (Å)	As_2O_5 (Å)
as received	17	25	25
freshly HCl etched	–	–	–
P1 (HCl etch)	14	24	24
P2 (HCl etch)	15	22	23
P3 (HCl etch)	15	23	23
P4 (HCl etch)	13	21	21
P5 (HCl etch)	15	23	23
freshly Br_2 etched	10	17	17
P1 (Br_2 etch)	15	22	22
P2 (Br_2 etch)	14	22	22
P3 (Br_2 etch)	16	23	23
P4 (Br_2 etch)	13	22	22
P5 (Br_2 etch)	16	24	24

Passivation. Passivation of semiconductor surfaces is a critical parameter of semiconductor device design. The main goal of surface passivation is to prevent the regrowth of the oxide layer on semiconductor surfaces, which can have a detrimental effect on electronic stability. Alkanethiols,[3−8] bifunctional amine/thiol molecules,[38] thioamides,[6,39] and amino acids[37] have all been used previously to passivate InAs surfaces. The passivation abilities of the peptides were determined in two separate ways. First, the ratio of oxide to nonoxide components present in the XPS spectra of each sample was analyzed. Second, the oxide layer thickness of each sample was estimated using the ratio of oxide to nonoxide components while accounting for the attenuation of the substrate photoelectrons through the oxide layer. Put together, both approaches provide sufficient evidence for determining the passivation abilities of the peptides. As described above, the Br_2 etch successfully removes the native oxide layer present on InAs based on the ratios of the oxide to nonoxide components. Therefore, by assuming that the as received sample is fully oxidized, the passivation ability of the peptides can be assessed by comparing the oxide to nonoxide ratios of the

dx.doi.org/10.1021/la104963v |*Langmuir* 2011, 27, 3774–3782

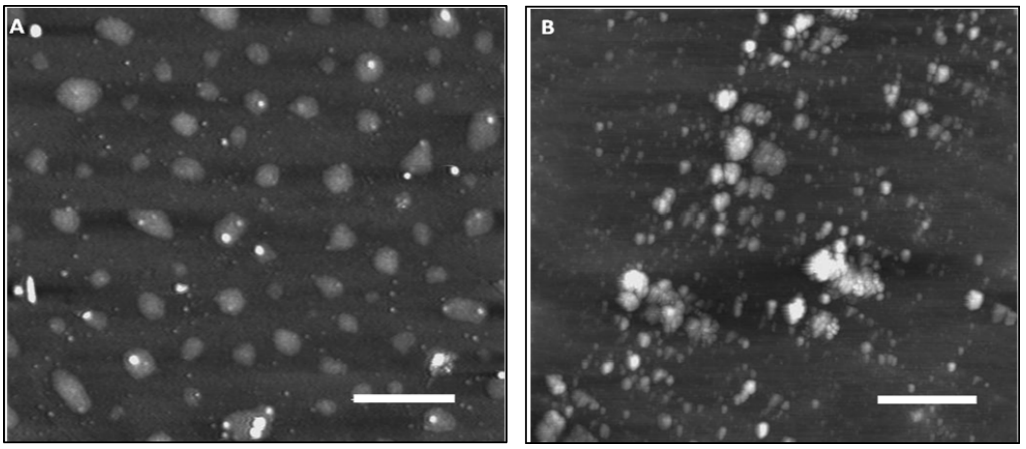

Figure 8. AFM images of peptide clusters on InAs surfaces functionalized with peptide P2 (GCGGELYASILY): (A) HCl etch and (B) Br_2 etch. Scale bar represents 500 nm.

peptide-functionalized samples to the as received and freshly Br_2-etched samples (Table 1). As expected, the as received sample had the highest oxide to nonoxide ratio, and the freshly Br_2-etched sample had the lowest oxide to nonoxide ratio. The ratios for the peptide-functionalized samples were significantly higher than the Br_2-etched sample for all photoemission lines, indicating that regrowth of the oxide layer did occur. However, the ratios do not reach the as received levels, indicating that the peptides have some passivation effect on the InAs surface.

The oxide to nonoxide method is a relatively rough and qualitative method of assessing passivation. Therefore, the passivation ability of the peptides on InAs was also analyzed by calculating the thickness of the oxide layer using the In 3d and As 3d spectra. For the oxide thickness calculations, the oxide layer was modeled as a semi-infinite substrate with a uniform overlayer as outlined by Fadley[34] in the following equation (for complete derivation, see the Supporting Information):

$$t = \Lambda_e^{\text{oxide}}(E_s) \ln\left(\frac{N_{\text{oxide}}(\theta)\rho_{\text{subst}}\Lambda_e^{\text{subst}}(E_s)}{N_{\text{subst}}(\theta)\rho_{\text{oxide}}\Lambda_e^{\text{oxide}}(E_s)} + 1\right) \quad (2)$$

In this case, $N_{\text{oxide}}(\theta)$ is the intensity of the In_2O_3, As_2O_3, or As_2O_5 components in the In 3d and As 3d spectra; $N_{\text{subst}}(\theta)$ is the intensity of the of In−As component in the In 3d spectra or the intensity of the As−In component in the As 3d spectra; ρ_{oxide} is the atomic density of indium or arsenic atoms present in In_2O_3, As_2O_3, or As_2O_5; ρ_{subst} is the atomic density of indium or arsenic present in the substrate; t is the thickness of the uniform oxide overlayer; and $\Lambda_e^{\text{oxide}}(E_s)$ and $\Lambda_e^{\text{subst}}(E_s)$ are the QEALs of the In 3d or As 3d photoelectrons through the oxide layer and InAs, respectively. Since the oxide layer consists of three separate components, As_2O_3, As_2O_5, and In_2O_3, the QEALs are estimated to account for the different concentration of oxides using the following equation:

$$\Lambda_e^{\text{oxide}}(E_s) = \alpha\Lambda_e^{As_2O_3}(E_s) + \beta\Lambda_e^{As_2O_5}(E_s) + \gamma\Lambda_e^{In_2O_3}(E_s) \quad (3)$$

Where α, β, and γ are correction factors that represent percent atomic concentrations of the As_2O_3, As_2O_5, and In_2O_3 components as calculated from each sample's As 3d and In 3d spectra. Oxides were supposed to be homogeneously blended, so ρ_{oxide} was also adjusted using the correction factors. Table 4 summarizes the oxide layer thicknesses for all samples based on the In 3d and As 3d photoemission lines, using the In_2O_3, As_2O_3, or As_2O_5 component intensities. The approximate oxide thicknesses range from 10 to 17 Å for those calculated by the In_2O_3 intensities and from 17 to 25 Å for those calculated by the As_2O_3 and As_2O_5 intensities. Since we assumed that the oxide layer was homogenously mixed, and since we accounted for the different atomic concentrations of the oxide components, it is expected that the oxide layer thicknesses would be similar. As seen in Table 4, the oxide thicknesses for the As 3d spectra are higher than for the In 3d spectra. However, for both photoemission lines, the oxide layer thickness was lowest for the freshly Br_2-etched sample and highest for the as received sample. The peptide samples did show oxide regrowth, as seen by the increase in oxide thicknesses when compared to the freshly Br_2-etched sample; however, the oxide thicknesses of the peptide samples did not reach the thicknesses seen by the as received sample.

The fact that both the oxide ratios and the oxide layer thicknesses did not reach the as received levels gives evidence that the peptides do have some passivation ability on InAs. The passivation ability of peptides is less when compared to the passivation ability of more commonly used molecules such as alkanethiol SAMs. Such SAMs have a higher affinity for InAs and form consistent monolayers on the surface, which block oxide regrowth to a high degree. Previous AFM studies suggest that peptides do not form consistent monolayers but agglomerate to form clusters on semiconductor surfaces.[27,28] Tapping mode AFM images of our peptide-functionalized surfaces indicate similar peptide cluster formation (Figure 8). Most likely, the area where the peptide adsorbed and clustered prevented the oxide regrowth, while oxide regrowth occurred on the bare InAs between the peptide clusters. It is important to note that we make the assumption that the peptide is able to adsorb onto the InAs surface before the oxide layer reforms. Because the adsorption reaction takes place in aqueous solution, it is possible that the oxide layer forms initially, and the peptide adsorption follows. However, if the peptide had adsorbed onto the oxide layer, the In 3d and As 3d would not have shown a decrease in the oxide to nonoxide ratio, since both the In 3d and As 3d photoelectrons penetrate relatively deeply into the surface. This decrease in oxide to nonoxide ratios for peptide-functionalized samples suggests that the peptides adsorb directly to InAs.

The peptides used in this study were not screened for affinity for semiconductor binding beforehand, so it is difficult to say whether or not the affinity of the peptides for the InAs surface directly affects the passivation ability of peptides. Previous reports show a relationship between peptide cluster size and peptide/semiconductor affinity, with low-affinity peptides forming fewer, larger clusters on the surface and high-affinity peptides forming many smaller clusters, presumably because of the higher affinity for peptide/peptide adhesion than peptide/semiconductor adhesion.[27,28] It is possible that the differences in peptide cluster size and quantity could potentially modulate the passivation effect seen by peptides on semiconductor substrates. Further studies would need to be performed in order to determine whether or not passivation depends on peptide affinity.

CONCLUSIONS

In this report, we assessed the adsorption and passivation ability of five different peptides on InAs surfaces using XPS. Before peptide functionalization, Br_2- and HCl-based etches were used to remove the native oxide layer and expose the bare InAs. The Br_2 etch successfully removed the oxide layer based on oxide to nonoxide ratios and confirmed by oxide layer thickness approximations. The HCl etch displayed significant contamination in the form of elemental arsenic, sulfur oxides, and nitrogen oxides, most likely due to the low postetch anneal temperature. The presence of amide components in the N 1s spectra of the peptide-functionalized samples showed that peptides successfully adsorbed on the InAs surface, regardless of the type of etch. The C 1s spectra and N 1s spectra were used to approximate peptide adlayer coverage in terms of peptide molecules per indium or arsenic atom. The C 1s spectra were deconvoluted based on peptide atomic structure. The peptide coverages range from ~20 to 40% of a monolayer for the C 1s spectra and from ~2 to 5% of a monolayer for the N 1s spectra. The difference in the coverage is attributed to the presence of carbon oxide contamination. After ensuring the peptides were adsorbed on the surfaces, the passivation ability of the peptides was analyzed using oxide to nonoxide ratios along with approximations of the oxide layer thicknesses. The approximate oxide thicknesses range from 10 to 17 Å, as calculated with the In_2O_3 components, and from 17 to 25 Å for the As_2O_3 and As_2O_5 components. Both the intensity ratios and the oxide layer thicknesses were consistently lower for the peptide-functionalized samples when compared to the as received samples, indicating that the peptides do have some passivation ability on InAs. The decreases in the oxide to nonoxide ratios also suggest that the peptides adsorb directly onto the InAs and not onto the oxide layer.

ASSOCIATED CONTENT

Supporting Information. Additional information on the quantitative analysis of the XPS spectra. This material is available free of charge via the Internet at http://pubs.acs.org.

AUTHOR INFORMATION

Corresponding Author
*E-mail: albena@purdue.edu.

ACKNOWLEDGMENT

The authors thank Drs. Alyssa Panitch and John Paderi for donating the peptides.

REFERENCES

(1) Dayeh, S. A. *Semicond. Sci. Technol.* **2010**, *25*, 1–20.
(2) Dayeh, S. A.; Soci, C.; Bao, X. Y.; Wang, D. L. *Nano Today* **2009**, *4*, 347–358.
(3) Petrovykh, D. Y.; Yang, M. J.; Whitman, L. J. *Surf. Sci.* **2003**, *523*, 231–240.
(4) Knoben, W.; Brongersma, S. H.; Crego-Calama, M. *J. Phys. Chem. C* **2009**, *113*, 18331–18340.
(5) Petrovykh, D. Y.; Smith, J. C.; Clark, T. D.; Stine, R.; Baker, L. A.; Whitman, L. J. *Langmuir* **2009**, *25*, 12185–12194.
(6) Petrovykh, D. Y.; Sullivan, J. M.; Whitman, L. J. *Surf. Interface Anal.* **2005**, *37*, 989–997.
(7) Hang, Q. L.; Wang, F. D.; Carpenter, P. D.; Zemlyanov, D.; Zakharov, D.; Stach, E. A.; Buhro, W. E.; Janes, D. B. *Nano Lett.* **2008**, *8*, 49–55.
(8) Tanzer, T. A.; Bohn, P. W.; Roshchin, I. V.; Greene, L. H.; Klem, J. F. *Appl. Phys. Lett.* **1999**, *75*, 2794–2796.
(9) Flores-Perez, R.; Zemlyanov, D. Y.; Ivanisevic, A. *ChemPhysChem* **2008**, *9*, 1528–1530.
(10) Mohaddes-Ardabili, L.; Martinez-Miranda, L. J.; Salamanca-Riba, L. G.; Christou, A.; Silverman, J.; Bentley, W. E.; Al-Sheikhly, M. *J. Appl. Phys.* **2004**, *95*, 6021–6024.
(11) Mohaddes-Ardabili, L.; Martinez-Miranda, L. J.; Silverman, J.; Christou, A.; Salamanca-Riba, L. G.; Al-Sheikhly, M.; Bentley, W. E.; Ohuchi, F. *Appl. Phys. Lett.* **2003**, *83*, 192–194.
(12) Lee, S. W.; Mao, C. B.; Flynn, C. E.; Belcher, A. M. *Science* **2002**, *296*, 892–895.
(13) Mao, C. B.; Flynn, C. E.; Hayhurst, A.; Sweeney, R.; Qi, J. F.; Georgiou, G.; Iverson, B.; Belcher, A. M. *Proc. Natl. Acad. Sci. U. S. A.* **2003**, *100*, 6946–6951.
(14) Shenton, W.; Douglas, T.; Young, M.; Stubbs, G.; Mann, S. *Adv. Mater.* **1999**, *11*, 253–256.
(15) Berti, L.; D'Agostino, P. S.; Boeneman, K.; Medintz, I. L. *Nano Research* **2009**, *2*, 121–129.
(16) Braun, E.; Eichen, Y.; Sivan, U.; Ben-Yoseph, G. *Nature* **1998**, *391*, 775–778.
(17) Medintz, I. L.; Berti, L.; Pons, T.; Grimes, A. F.; English, D. S.; Alessandrini, A.; Facci, P.; Mattoussi, H. *Nano Lett.* **2007**, *7*, 1741–1748.
(18) Bai, H. Y.; Xu, F.; Anjia, L.; Matsui, H. *Soft Matter* **2009**, *5*, 966–969.
(19) Banerjee, I. A.; Yu, L. T.; Matsui, H. *Proc. Natl. Acad. Sci. U. S. A.* **2003**, *100*, 14678–14682.
(20) Behrens, S.; Wu, J.; Habicht, W.; Unger, E. *Chem. Mater.* **2004**, *16*, 3085–3090.
(21) Djalali, R.; Chen, Y. F.; Matsui, H. *J. Am. Chem. Soc.* **2003**, *125*, 5873–5879.
(22) Gao, F.; Lu, Q. Y.; Meng, X. K.; Komarneni, S. *J. Phys. Chem. C* **2008**, *112*, 13359–13365.
(23) Reches, M.; Gazit, E. *Science* **2003**, *300*, 625–627.
(24) Whaley, S. R.; English, D. S.; Hu, E. L.; Barbara, P. F.; Belcher, A. M. *Nature* **2000**, *405*, 665–668.
(25) Trentler, T. J.; Hickman, K. M.; Goel, S. C.; Viano, A. M.; Gibbons, P. C.; Buhro, W. E. *Science* **1995**, *270*, 1791–1794.
(26) Wang, F.; Dong, A.; Sun, J.; Tang, R.; Yu, H.; Buhro, W. E. *Inorg. Chem.* **2006**, *45*, 7511–7521.
(27) Goede, K.; Busch, P.; Grundmann, M. *Nano Lett.* **2004**, *4*, 2115–2120.
(28) Goede, K.; Grundmann, M.; Holland-Nell, K.; Beck-Sickinger, A. G. *Langmuir* **2006**, *22*, 8104–8108.
(29) Paderi, J. E.; Panitch, A. *Biomacromolecules* **2008**, *9*, 2562–2566.
(30) Millea, M. F.; McColl, M.; Silver, A. H. *J. Electron. Mater.* **1976**, *5*, 321–340.
(31) Tereshchenko, O. E.; Paget, D.; Chiaradia, P.; Bonnet, J. E.; Wiame, F.; Taleb-Ibrahimi, A. *Appl. Phys. Lett.* **2003**, *82*, 4280–4282.
(32) Tereshchenko, O. E.; Placidi, E.; Paget, D.; Chiaradia, P.; Balzarotti, A. *Surf. Sci.* **2004**, *570*, 237–244.
(33) Jedlicka, S. S.; Rickus, J. L.; Zemlyanov, D. Y. *J. Phys. Chem. B* **2007**, *111*, 11850–11857.

(34) Fadley, C. S. In *Electron Spectroscopy, Theory, Techniques, and Applications*; Brundle, C. R., Baker, A. D., Eds.; Academic Press: London, 1978; Vol. 11, pp 71−75.
(35) Jablonski, A.; Powell, C. J. *Surf. Sci. Rep* **2002**, *47*, 35–91.
(36) NIST Electron Effective-Attenuation-Length Database, Version 1.2. In *NIST Standard Reference Database 82*; National Institutes of Standards and Technology: Gaithersburg, MD, 2009.
(37) Slavin, J. W. J.; Jarori, U.; Zemlyanov, D.; Ivanisevic, A. *J. Electron Spectrosc. Relat. Phenom.* **2009**, *172*, 47–53.
(38) Stine, R.; Petrovykh, D. Y. *J. Electron Spectrosc. Relat. Phenom.* **2009**, *172*, 42–46.
(39) Stine, R.; Aifer, E. H.; Whitman, L. J.; Petrovykh, D. Y. *Appl. Surf. Sci.* **2009**, *255*, 7121–7125.